THE JOURNAL OF PHYSICAL CHEMISTRY B

ARTICLE

pubs.acs.org/JPCB

Gating of a Water Nanochannel Driven by Dipolar Molecules

X. W. Meng,[†] Y. Wang,[†] Y. J. Zhao,[*,‡] and J. P. Huang[*,†]

[†]Department of Physics and State Key Laboratory of Surface Physics, Fudan University, Shanghai 200433, China

[‡]Advanced Materials Laboratory, Fudan University, Shanghai 200438, China

ABSTRACT: On the basis of molecular dynamics simulations, we investigate water permeation across a single-walled carbon nanotube (SWCNT) under the influence of four symmetrical half-rings, each having six LiF dipolar molecules. The flux remains almost fixed as the separation, R, between the rings and SWCNT is larger than 1.562 nm, but decreases significantly as 0.944 nm < R < 1.562 nm, and reaches zero as R < 0.944 nm. This nanochannel shows an excellent on−off gate that is both effectively resistant to dipole noises and sensitive to available signals. The finite element method reveals that the electrostatic field generated by LiF molecules plays a unique role in achieving the gating of the water SWCNT. Each water molecule tends to stay at the most stable state by moving to the location with the highest field strength in order to maintain its lowest electric energy. These findings may have biological implications because membrane water nanochannels made up of proteins accompanied with co-ions and counterions (due to ionization) share a similar single-file water chain inside the SWCNT with dipoles. The Appendix shows a possible link between the model system and a membrane water nanochannel with co-ions and counterions. Furthermore, our observations may have significance for the design of SWCNT-based nanoscale devices with dipolar molecules.

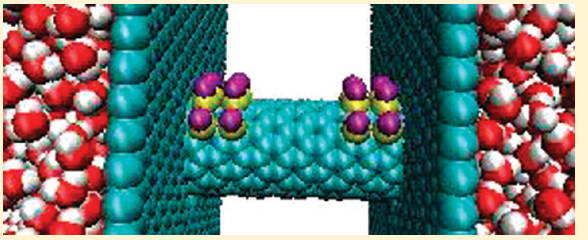

INTRODUCTION

It is known that the transportation of water molecules across water nanochannels in membranes plays an important role in biological activities.[1−10] Water permeation through membranes can be regulated by pH,[11,12] solute concentration,[13,14] and temperature.[15,16] However, the complex structure of biological water nanochannels and protein−water interactions often make further investigations of the mechanism of such nanochannels very complicated. It has been well recognized that carbon nanotubes can be used as model systems to exploit some of the primary behavior of the biological water nanochannels.[17−19] Hummer et al. showed that single-walled carbon nanotubes (SWCNT) can be designed as nanochannels for water molecules;[19] they observed that a minute reduction in the attraction between the tube wall and water dramatically affected pore hydration, leading to sharp two-state transitions between empty and filled states on a nanosecond time scale.

Biological water nanochannels are usually gated. They contain a region that can interrupt the flow of water molecules and thus can switch between on and off states. This region plays a crucial role in water permeation across a biological membrane. Wan et al. have studied that an on−off gating behavior can be realized by adding an external force on the carbon nanotube.[9] In their consideration, the origin of the force can be seen to originate from effective techniques and/or other molecules. Furthermore, an on−off gating behavior of water nanochannels was also revealed by using a single external charge of value +1.0e,[20] in order to study the response to the indispensable charges as well as the possible charge noise near water nanochannels, as inspired from charged residues in nanochannel proteins such as aquaporin.[8] Their study[20] utilizes the interaction between a point charge outside the SWCNT and charge-neutral water molecules inside. Despite the existing achievements,[20] the dependence of the gating of a water nanochannel on charges is still far from being well understood. In particular, due to ionization, co-ions (and thus counterions) are indispensable in membrane proteins (and physiological solutions inside and outside the cells). In detail, ionization can cause membrane proteins to have co-ions with either negative or positive charges, which depends on the pH value of the host solution. Owing to the principle of electric neutrality, the electric quantity of co-ions in membrane proteins exactly cancels that of counterions in physiological solutions. In this work, a SWCNT with dipoles is used as a prototype to study the response to the indispensable co-ions and counterions. It is worth mentioning that Leung[21] elucidated the dramatic effect of dipolar layers on electrolyte permeation by investigating the electrostatic potential generated by radically aligned surface dipoles along nanopores. As a result, he revealed the role of dipoles in patterned ion distributions. Clearly, this is due to the interaction between dipoles and charged ions. In contrast, here we consider the interaction between dipoles and uncharged water molecules. Accordingly, this work also provides the possibility of controlling the water flow across the SWCNT and developing SWCNT-based nanoscale devices by applying dipolar molecules appropriately.

METHODOLOGY

Molecular dynamics, which has been used widely for the studies of water dynamics in SWCNTs, proteins, and in-between proteins,[19,20,22−38] is adopted here for this work. Our simulation framework is shown in Figure 1; two parallel graphite sheets with

Received: March 17, 2011
Published: April 05, 2011

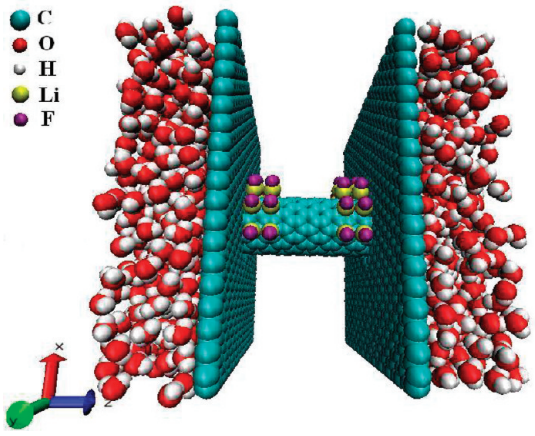

Figure 1. Snapshot of the simulation system with a Z-directed SWCNT perpendicularly joining the centers of two graphite sheets. The system is filled by water molecules (H_2O). Four half-rings, each having six lithium fluoride (LiF) dipolar molecules, are symmetrically positioned along radial direction of the SWCNT. Besides atom C, the atoms of H_2O and LiF are shown in different colors. More details, e.g., the positions of the four half-rings, can be found in the main text. For a possible link between this system and a membrane water nanochannel with co-ions and counterions, please refer to the Appendix for a qualitative demonstration.

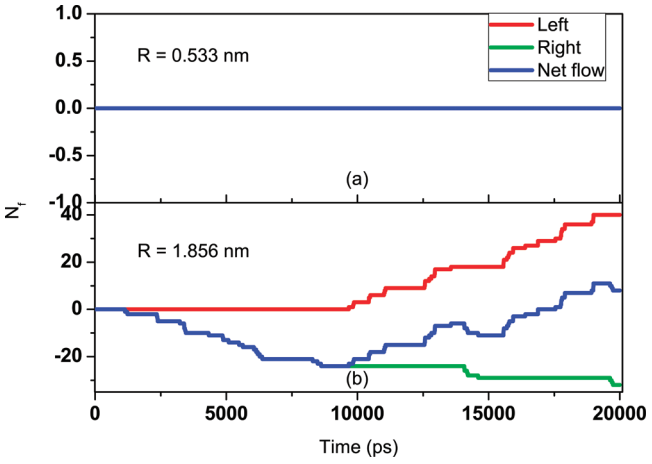

Figure 2. Number of water molecules, N_f, flowing across the SWCNT as a function of time (with step size 2 fs) for two R's (the separation between the rings and SWCNT): (a) R = 0.533 nm and (b) R = 1.856 nm. "Left" (or "Right") denotes the water flow from the left (or right) side of the SWCNT to the right (or left) side, and "Net flow" means the difference between the numbers of water molecules leaving from one end and the other. We define the number of water molecules transporting from left to right is positive, and that from right to left is negative. The three curves in (a) are overlapped.

a separation of 2.680 nm dividing the full space into three parts. A Z-directed, uncapped, (10, 0) SWCNT with diameter 0.772 nm is used to perpendicularly join the two graphite sheets. The Lennard-Jones potential parameters arrive from Hummer et al.[19] The SWCNT and graphite sheets are solvated in a water box (4.652 nm × 4.646 nm × 5.000 nm) with 1549 water molecules. The model for TiP3P water molecules is used.[39] Periodic boundary conditions are applied in all directions. The two ends of the SWCNT are located at Z = 1.310 and 3.690 nm, respectively. The four half-rings, each having six LiF dipolar molecules, are located at Z = 1.590, 1.890, 3.110, and 3.410 nm, respectively. Here, LiF molecules are used as model dipolar molecules whose unique features have long been discussed.[40,41] We place each LiF molecule along the radial direction of the SWCNT, with the Li atoms closer to the SWCNT than F atoms, and the four half-rings of LiF molecules along the Z direction; see Figure 1. The angle between two adjacent LiF molecules in each half-ring is 36°, and the dipole moment for LiF molecules is 6.294 D (1 D ≈ 3.335 64 × 10^{-30} C·m).[42] To prevent the SWCNT and graphite sheets being swept away, all of the C atoms were fixed in the simulations.

We perform molecular dynamics simulations with Gromacs 3.3.1, and adopting the thermostat of Berendsen et al.[43] with a time constant of 0.5 ps. In our simulations, a time step of 2 fs in an NVT ensemble at temperature 300 K is used and the particle-mesh Ewald method[44] with a real space cutoff of 1 nm is utilized to treat long-range interactions.

RESULTS

Figure 2 shows the number of water molecules, N_f, flowing across the SWCNT as a function of time for two positions of R. Here, R denotes the smallest distance between an Li atom and the centerline of the SWCNT. For instance, R = 0.533 nm corresponds to the distance 0.147 nm between an Li atom and the nearest C atom in the SWCNT. From Figure 2a, we find that no water permeation across the SWCNT appears for R = 0.533 nm. Clearly, R = 0.533 nm corresponds to an off state of the SWCNT where water molecules cannot transport through it. In contrast, for R = 1.856 nm, water permeation appears either from right to left or from left to right. This corresponds to an on state of the SWCNT which allows water molecules to transport. Therefore, Figure 2 shows an on−off gating behavior of the SWCNT with dipoles by choosing appropriate values of R. Here, we should remark that, even though the net flow for R = 1.856 nm within the simulation time 20 ns is nonzero, due to the symmetry between the water flow from left to right and that from right to left, it should tend to zero as long as the simulation time is long enough.

To further understand Figure 2, in Figure 3 we display the average orientation of water molecules inside the SWCNT, in the presence of the external dipoles. Here the orientation is defined as the average angle, $\langle\phi(t)\rangle$, at time t

$$\langle\phi(t)\rangle = \sum_{i=1}^{N} \phi_i(t)/N(t) \quad (1)$$

where $N(t)$ is the number of water molecules and $\phi_i(t)$ denotes the angle between $\vec{\mu}_i$ (dipole moment of the ith water molecule) and $\hat{u}$ (axis unit vector of the SWCNT) according to

$$\phi_i(t) = \arccos(\vec{\mu}_i \cdot \hat{u}/|\vec{\mu}_i|) \quad (2)$$

The four half-rings of LiF molecules divide the Z-directed SWCNT into five regions, namely, region 1 for Z = 1.310−1.590 nm, region 2 for Z = 1.590−1.890 nm, region 3 for Z = 1.890−3.110 nm, region 4 for Z = 3.110−3.410 nm, and region 5 for Z = 3.410−3.690 nm. Here, region i (i = 1, 2, 3, 4, and 5) contains an average orientation of water molecules, denoted by angle i, given by $\langle\phi(t)\rangle$ (eq 1). In the case of the off state (R = 0.533 nm) as shown in Figure 3a, average orientations of water molecules are tilted from angle 1 to angle 5. Incidentally, angle 1 (or 2) is statistically equal to angle 5 (or 4), due to the symmetry structure of the four half-rings of LiF molecules. On the other hand, the orientation behavior of water molecules for

dx.doi.org/10.1021/jp2025297 |J. Phys. Chem. B 2011, 115, 4768–4773

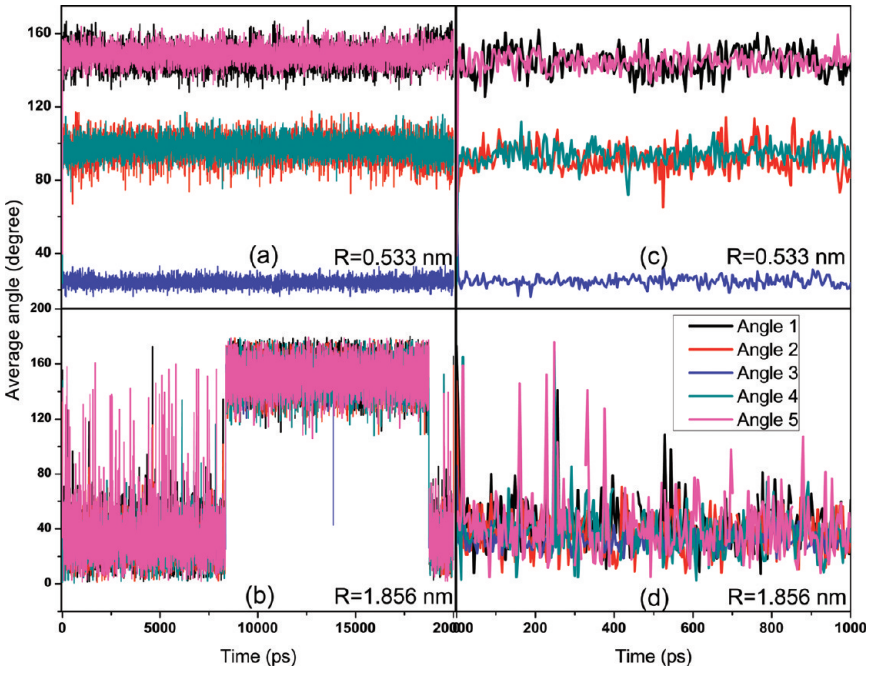

Figure 3. Average orientations (angles 1−5) of water molecules inside the SWCNT as a function of time for two positions of R: (a) R = 0.533 nm and (b) R = 1.856 nm. Panels c and d show the details corresponding to the first 1000 ps in panels a and b, respectively. The definition for angles 1−5 can be found in the main text.

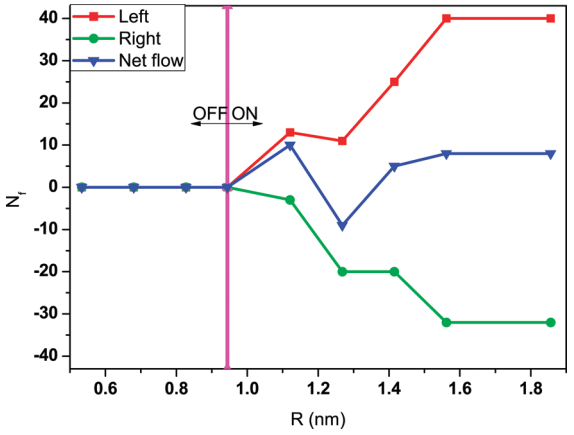

Figure 4. Number of water molecules, N_f, flowing across the SWCNT within 20 ns as a function of R. Others are the same as Figure 2.

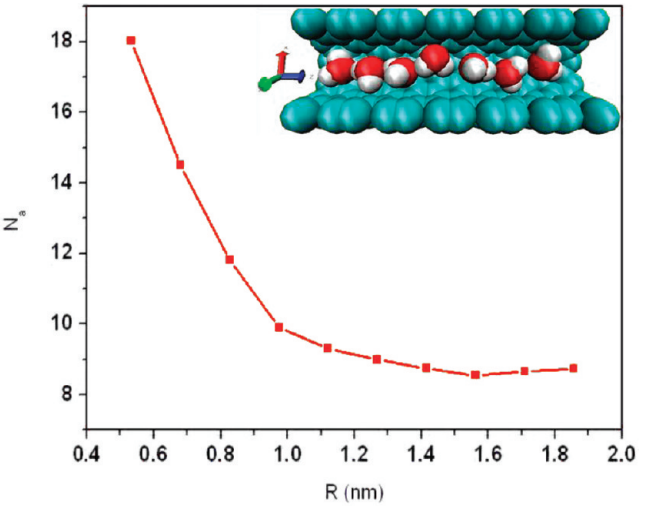

Figure 5. Average number of water molecules, N_a, confined in the SWCNT within 20 ns as a function of R. The line is a guide to the eye.

the on state (R = 1.856 nm) in Figure 3b is quite different from that in Figure 3a. Angles 1−5 in Figure 3b are statistically equal to each other. The orientation of water molecules has sharp transitions as the simulation time increases. Additionally, for clarity, the details corresponding to the first 1000 ps in Figure 3a (or b) are displayed in Figure 3c (or d), where the relation among angles 1−5 is displayed clearly. In conclusion, Figure 3 clearly displays that orientations of water molecules are also sensitive to the signal of LiF molecules.

As an extension of Figure 2, where only two R's are plotted, Figure 4 shows a general case where the number of water molecules, N_f, flowing across the SWCNT is presented as R varies from 0.533 to 1.856 nm. It is found that N_f is always zero as R < 0.944 nm, which thus corresponds to an off state of the SWCNT. In contrast, as R > 0.944 nm, N_f becomes nonzero, which is related to an on state of the SWCNT. It is also worth noting that the effect of LiF molecules on the flow across the SWCNT is found to be negligible when R > 1.562 nm. However, for 0.944 nm < R < 1.562 nm, this effect plays an evident role. Particularly, Figure 5 shows the average number of water molecules, N_a, confined in the SWCNT. We find that increasing R decreases N_a. Furthermore, when R > 1.415 nm, N_a is almost constant. This can be understood; when the LiF molecules are away enough from the SWCNT, their interaction with the water molecules can be neglected.

To reveal the physical mechanism underlying the above-mentioned on−off gating phenomena, we utilize the finite element method[45] for studying two-dimensional (2D) electrostatic

dx.doi.org/10.1021/jp2025297 |J. Phys. Chem. B 2011, 115, 4768–4773

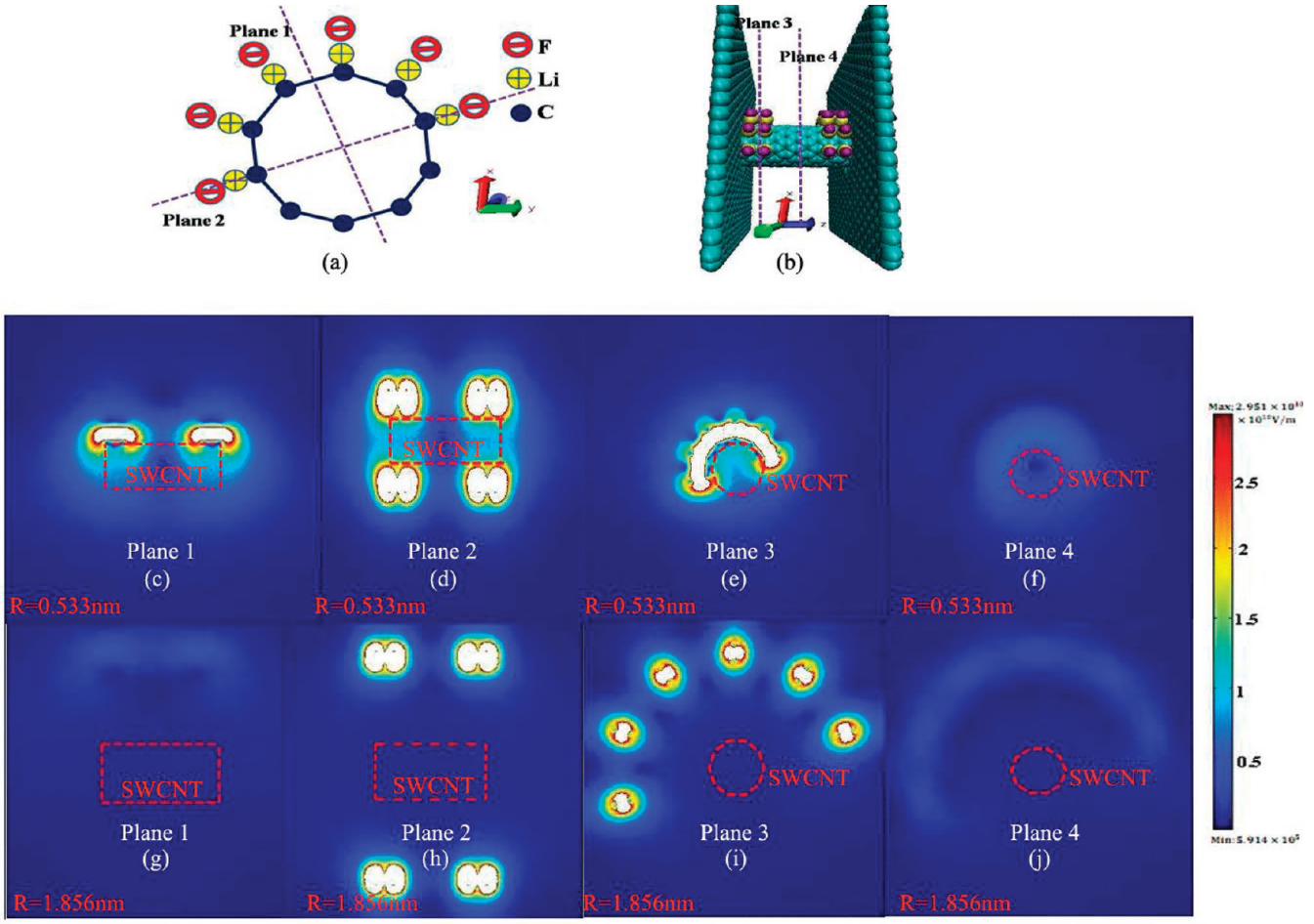

Figure 6. Schematic graphs showing four two-dimensional (2D) virtual planes in the simulation system: (a) planes 1 and 2, and (b) planes 3 and 4. The finite element method is performed to show the 2D electrostatic field strength distribution in (c,g) plane 1, (d,h) plane 2, (e,i) plane 3, and (f,j) plane 4, for (c−f), $R = 0.533$ nm and (g−j), $R = 1.856$ nm. In (c−j), the white regions possess the value of the electric field strengths exceeding the bounds of bars. Both the dashed rectangle in (c,d,g,h) and the dashed circle in (e,f,i,j) denote the position of the SWCNT.

field strength distributions in the simulation system; see Figure 6. In particular, we investigated the field distributions in the four 2D virtual planes as indicated in Figure 6, a and b. The result is shown in Figure 6c−j. For R = 0.533 nm, we find that the field distribution is quite inhomogeneous inside the SWCNT, and the area close to the LiF molecules has a higher field strength, E. In contrast, for R = 1.856 nm, the field distribution inside the SWCNT is much more homogeneous and the field strength is relatively low. According to electrodynamics, if one puts the ith water molecule with dipole moment $\vec{\mu}_i$, the water molecule will tend to move to the area with the highest field strength, in order to maintain the lowest electric energy determined by $-\vec{\mu}_i \cdot E$. To clarify this, when the LiF molecules are located close to the SWCNT (say $R = 0.533$ nm), the field strength generated by LiF will increase inside the SWCNT, thus attracting water molecules more strongly. As a result, the on or off state can be achieved for the SWCNT by appropriately choosing the position, R, of dipolar molecules. This can explain the mechanism underlying the on (or off) state of the SWCNT when the LiF molecules are away from (or close to) the SWCNT (as obtained in Figures 2 and 4), and can also explain the results obtained in Figure 5, where the average number of water molecules confined in the SWCNT decreases as the LiF molecules move away.

DISCUSSION AND CONCLUSION

Here some comments are in order. The geometric design of molecules (say, half-rings) and number of molecules/half-rings can change quantitative results (say, angle distributions as displayed in Figure 3), rather than qualitative results, namely, gating behavior. It is because the only requirement for achieving the gating behavior is that the local electric field acting on the water molecules inside the nanotube should be strong enough. In this sense, the screening or image charge effect does not affect the gating behavior either because one may overcome the weakening effect caused by this effect by adding more dipolar molecules into the system accordingly. Thus, for convenience, we have omitted the effect of screening or image charges in the simulations.

To sum up, using molecular dynamics simulations, we have investigated water permeation across a SWCNT surrounded by four half-rings of LiF dipolar molecules arranged in a symmetrical structure. The designed system shows an excellent on−off gating behavior; it is in the on/off state when the distance between LiF and the SWCNT is larger/smaller than a critical distance of 0.944 nm. In this system, the dipolar effect on the flow across the SWCNT is found to be negligible when the distance is greater than 1.562 nm. The finite element method helps us reveal that

dx.doi.org/10.1021/jp2025297 |J. Phys. Chem. B 2011, 115, 4768–4773

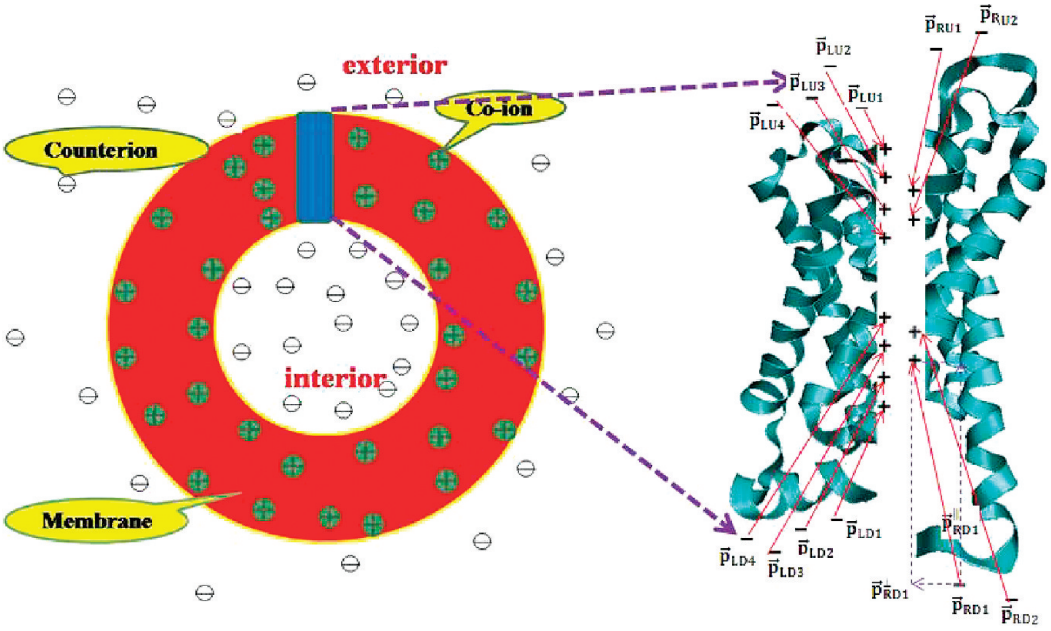

Figure 7. Schematic graph showing a cell membrane shaded red in the left panel. Here cations serve as co-ions (plus symbols), and anions are counterions (minus symbols). A biological water nanochannel made up of proteins are shaded blue on the left, and schematically shown on the right. Each pair of co-ion and counterion is modeled as a dipole (red solid arrow) with a moment $\mathbf{p}$ which can be separated into the parallel ($\parallel$) and perpendicular ($\perp$) parts, say $\mathbf{p}_{RD1} = \mathbf{p}^{\parallel}_{RD1} + \mathbf{p}^{\perp}_{RD1}$. Here 12 moments, $\mathbf{p}$, are schematically indicated on the right.

the electrostatic field generated by LiF molecules plays a unique role in achieving the gating of the water SWCNT, as each water molecule tends to stay at the most stable state by moving to the location with the highest field strength in order to maintain its lowest electric energy. These findings may have biological implications because membrane water nanochannels made up of proteins with co-ions and counterions share a similar single-file water chain inside the SWCNT with dipoles. Also, our observations may have significance for the design of SWCNT-based nanoscale devices with dipolar molecules that are abundant in nature.

APPENDIX: A POSSIBLE LINK BETWEEN OUR MODEL SYSTEM AND A MEMBRANE WATER NANOCHANNEL

A membrane water nanochannel consists of proteins that can be charged by ionization. Proteins can be either negatively or positively charged, depending on the pH value of the host solution. Figure 7 shows a schematic graph for a cell membrane region (shaded red in the left panel) and a membrane water nanochannel (right panel). As a model demonstration, here ionization is assumed to give membrane proteins positive charges (co-ions), and the interior/exterior regions negative charges (counterions). The right panel of Figure 7 shows an enlarged version of a water nanochannel, where each pair of co-ion and counterion is seen as a dipole moment p, as indicated by a red solid arrow. In order to bridge the nanochannel with our simulation system, we need to make two main assumptions:

Assumption 1. We assume the distribution of ions in the upper region of the nanochannel is nonsymmetrical, namely

$$\sum_{i=1}^{4} \mathbf{p}_{LUi} > \sum_{j=1}^{2} \mathbf{p}_{RUj} \tag{3}$$

Similarly, the same relation holds for the lower region:

$$\sum_{i=1}^{4} \mathbf{p}_{LDi} > \sum_{j=1}^{2} \mathbf{p}_{RDj} \tag{4}$$

Due to fluctuation of counterions in the real system, Assumption 1 could be somehow reasonable, which effectively corresponds to half-rings of dipoles used in our simulation system.

Assumption 2. All parallel components of the dipole moment are assumed to cancel, namely

$$\sum_{i=1}^{2} \mathbf{p}^{\parallel}_{RDi} + \sum_{j=1}^{4} \mathbf{p}^{\parallel}_{LDj} = \sum_{k=1}^{2} \mathbf{p}^{\parallel}_{RUk} + \sum_{l=1}^{4} \mathbf{p}^{\parallel}_{LUl} \tag{5}$$

Similarly, we set the perpendicular components of the dipole moments to satisfy

$$\sum_{i=1}^{2} \mathbf{p}^{\perp}_{RDi} + \sum_{j=1}^{4} \mathbf{p}^{\perp}_{LDj} = \sum_{k=1}^{2} \mathbf{p}^{\perp}_{RUk} + \sum_{l=1}^{4} \mathbf{p}^{\perp}_{LUl} \tag{6}$$

To some extent, assumption 2 agrees with our simulation system with the four half-rings arranged in symmetrical structure.

Additionally, in our simulation system a dipole moment with a fixed strength is used to model each pair of co-ion and counterion during water transportation. This could be reasonable, at least to some extent, because the speed for water molecules to cross through the nanochannel can be so high that each pair of co-ion and counterion may be stationary in the duration. For this, the statistical reason is that the counterions are bombarded by many water molecules surrounding them and that they are more difficult to move than water molecules travelling through the nanochannel which are only bombarded by two nearby water molecules in a single file.

According to the above analysis, under some conditions, we believe membrane water nanochannels with co-ions and counterions

dx.doi.org/10.1021/jp2025297 |J. Phys. Chem. B 2011, 115, 4768–4773

can be qualitatively modeled as a SWCNT surrounded with dipoles. However, this Appendix is by no means meant to strictly bridge our simulation system and a real biological water nanochannel, because the real situation is too complicated. Indeed, this work only offers a simplified research, but gives some hints on the gating of real water nanochannels with co-ions and counterions.

AUTHOR INFORMATION

Corresponding Author

*E-mail: zhaoyanjiao@fudan.edu.cn (Y.J.Z.); jphuang@fudan.edu.cn (J.P.H.).

ACKNOWLEDGMENT

We acknowledge the financial support by the National Natural Science Foundation of China under Grant Nos. 10874025 and 11075035, and by Chinese National Key Basic Research Special Fund under Grant No. 2011CB922004.

REFERENCES

(1) Denker, B. M.; Smith, B. L.; Kuhajda, F. P.; Agre, P. *J. Biol. Chem.* **1988**, *263*, 15634.
(2) Preston, G. M.; Agre, P. *Proc. Natl. Acad. Sci. U.S.A.* **1991**, *88*, 11110.
(3) Zeidel, M. L.; Ambudkar, S. V.; Smith, B. L.; Agre, P. *Biochemistry* **1992**, *31*, 7436.
(4) Murata, K.; Mitsuoka, K.; Hirai, T.; Walz, T.; Agre, P.; Heymann, J. B.; Engel, A.; Fujiyoshi, Y. *Nature* **2000**, *407*, 599.
(5) Miyazawa, A.; Fujiyoshi, Y.; Unwin, N. *Nature* **2003**, *423*, 949.
(6) Sui, H. X.; Han, B. G.; Lee, J. K.; Walian, P.; Jap, B. K. *Nature* **2001**, *414*, 872.
(7) Zhou, M.; Morais-Cabral, J. H.; Mann, S.; Mackinnon, R. *Nature* **2001**, *411*, 657.
(8) Agre, P. *Angew. Chem., Int. Ed.* **2004**, *43*, 4278.
(9) Wan, R. Z.; Li, J. Y.; Lu, H. J.; Fang, H. P. *J. Am. Chem. Soc.* **2005**, *127*, 7166.
(10) Gong, X. J.; Li, J. Y.; Lu, H. J; Wan, R. Z.; Li, J. C.; Hu, J.; Fang, H. P. *Nature Nanotechnol.* **2007**, *2*, 709.
(11) Iwata, H.; Matsuda, T. *J. Membr. Sci.* **1988**, *38*, 185.
(12) Ito, Y.; Park, Y. S.; Imanishi, Y. *Langmuir* **2000**, *16*, 5376.
(13) Osada, Y.; Honda, K.; Ohta, M. *J. Membr. Sci.* **1986**, *27*, 327.
(14) Yoshimi, Y.; Arai, R.; Nakayama, S. *Anal. Chim. Acta* **2010**, *682*, 110.
(15) Yang, M.; Xie, R.; Wang, J. Y.; Ju, X. J.; Yang, L. H.; Chu, L. Y. *J. Membr. Sci.* **2010**, *355*, 142.
(16) Lee, S. H.; Chung, G. C.; Steudle, E. *Plant Cell Environ.* **2005**, *28*, 1191.
(17) Andreev, S.; Reichman, D.; Hummer, J. P. *J. Chem. Phys.* **2005**, *123*, 194502.
(18) Zhu, F.; Schulten, K. *Biophys. J.* **2003**, *85*, 236.
(19) Hummer, G.; Rasaiah, J. C.; Noworyta, J. P. *Nature* **2001**, *414*, 188.
(20) Li, J. Y.; Gong, X. J.; Lu, H. J.; Li, D.; Zhou, R. H. *Proc. Natl. Acad. Sci. U.S.A* **2007**, *104*, 3687.
(21) Leung, K. *J. Am. Chem. Soc.* **2008**, *130*, 1808.
(22) de Groot, B. L.; Grubmuller, H. *Science* **2001**, *294*, 2353.
(23) Jensen, M. O.; Tajkhorshid, E.; Schulten, K. *Biophys. J.* **2003**, *85*, 2884.
(24) Pomés, R.; Roux, B. *Biophys. J.* **1998**, *75*, 33.
(25) de Groot, B. L.; Grubmuller, H. *Curr. Opin. Struct. Biol.* **2005**, *15*, 176.
(26) Kalra, A.; Garde, S.; Hummer, G. *Proc. Natl. Acad. Sci. U.S.A.* **2003**, *100*, 10175.
(27) Koga, K.; Gao, G. T.; Tanaka, H.; Zeng, X. C. *Nature* **2001**, *412*, 802.
(28) Zhou, R. H.; Huang, X. H.; Margulis, C. J.; Berne, B. J. *Science* **2004**, *305*, 1605.
(29) Liu, P.; Huang, X. H.; Zhou, R. H.; Berne, B. J. *Nature* **2005**, *437*, 159.
(30) Cheung, M. S.; Thirumalai, D. *J. Mol. Biol.* **2006**, *357*, 632.
(31) Fernandez, A.; Scheraga, H. A. *Proc. Natl. Acad. Sci. U.S.A.* **2003**, *100*, 113.
(32) Wallqvist, A.; Gallicchio, E.; Levy, R. M. *J. Phys. Chem. B* **2001**, *105*, 6745.
(33) Dill, K. A.; Chan, H. S. *Nat. Struct. Biol.* **1997**, *4*, 10.
(34) Cheng, Y.; Rossky, P. J. *Nature* **1998**, *392*, 696.
(35) Zuo, G.; Shen, R.; Ma, S.; Guo, W. *ACS Nano* **2010**, *4*, 205.
(36) Wong-ekkabut, J.; Miettinen, M. S.; Dias, C.; Karttunen, M. *Nature Nanotechnol.* **2010**, *5*, 555.
(37) Corry, B. *J. Phys. Chem. B* **2008**, *112*, 1427.
(38) Walther, J. H.; Jaffe, R.; Halicioglu, T.; Koumoutsakos, P. *J. Phys. Chem. B* **2001**, *105*, 9980.
(39) Jorgensen, W. L.; Chandrasekhar, J.; Madura, J. D.; Impey, R. W.; Klein, M. L. *J. Chem. Phys.* **1983**, *79*, 926.
(40) Wang, L. L.; Perera, A.; Cheng, H. P. *Phys. Rev. B* **2003**, *68*, 115409.
(41) Zhang, L.; Yan, S. H.; Cukier, R. I.; Bu, Y. X. *J. Phys. Chem. B* **2008**, *112*, 3767.
(42) Bader, R. F. W.; Henneker, W. H. *J. Am. Chem. Soc.* **1965**, *87*, 3063.
(43) Berendsen, H. J. C.; Postma, J. P. M.; Gunsteren, V.; Dinola, A.; Haak, J. R. *J. Chem. Phys.* **1984**, *81*, 3684.
(44) Darden, T. A.; York, D. M.; Pedersen, L. G. *J. Chem. Phys.* **1993**, *98*, 10089.
(45) Gao, Y.; Huang, J. P.; Liu, Y. M.; Gao, L.; Yu, K. W.; Zhang, X. *Phys. Rev. Lett.* **2010**, *104*, 034501.